LNF-96/074

Performance of the New Plastic Scintillator NE110A for the CLAS Large Angle Calorimeter

P. Rossi, E. Polli, M. Albicocco, H. Avakian, N. Bianchi, G.P. Capitani, A. Deppman, E. De Sanctis, V. Giourdjian, P. Levi Sandri, S. Mansanta, M. Mirazita, V. Muccifora, A.R. Reolon, M. Taiuti, A. Rottura, M. Anghinolfi, M. Battaglieri, P. Corvisiero, E. Golovach, A. Longhi, V.I. Mokeev, M. Olcese, G. Ricco, M. Ripani, M. Sanzone, V. Sapunenko, R. Morandotti

Nuclear Instruments & Methods A, 381, 32-38, (1996)

Nuclear Instruments and Methods in Physics Research A 381 (1996) 32–38

ELSEVIER

NUCLEAR INSTRUMENTS & METHODS IN PHYSICS RESEARCH Section A

Performance of the new plastic scintillator NE110A for the CLAS large angle calorimeter

P. Rossi[a], E. Polli[a], M. Albicocco[a], H. Avakian[a], N. Bianchi[a], G.P. Capitani[a], A. Deppman[a], E. De Sanctis[a,*], V. Giourdjian[a], P. Levi Sandri[a], S. Mansanta[a], M. Mirazita[a], V. Muccifora[a], A.R. Reolon[a], M. Taiuti[b], A. Rottura[b], M. Anghinolfi[b], M. Battaglieri[b], P. Corvisiero[b], E. Golovach[b], A. Longhi[b], V.I. Mokeev[b], M. Olcese[b], G. Ricco[b], M. Ripani[b], M. Sanzone[b], V. Sapunenko[b], R. Morandotti[c]

[a]*INFN-Laboratori Nazionali di Frascati. P.O. Box 13, I-00044, Frascati, Italy*
[b]*Dipartimento di Fisica dell'Università di Genova e INFN-Sezione di Genova, I-16146, Genova, Italy*
[c]*NE Technology, Edinburgh, Scotland, UK*

Received 15 May 1996

Abstract

The performance of the new NE110A plastic scintillator has been measured in connection with the construction of the AIACE large angle electromagnetic calorimeter for the CLAS detector at CEBAF. Measurements concerning 2128 scintillator bars 15 mm thick, roughly 10 cm wide and up to 450 cm length are reported. The results show an attenuation length of the order of 400 cm, a light output of ≥ 40 photoelectrons/MeV and a uniformity $> 98\%$.

1. Introduction

Particles produced in the experimental Hall B [1] at CEBAF will be measured by the Cebaf Large Acceptance Spectrometer (CLAS) [2]. The magnetic field of this spectrometer is generated by six superconducting coils which divide the detector into six sectors. Each sector is instrumented individually with detector subsystems to form six independent spectrometers. The forward region of these six sectors, corresponding to polar scattering angles between 8° and 45°, will be equipped with an electromagnetic shower calorimeter. For one of these six sectors, the coverage of the electromagnetic calorimeter will be extended to include polar scattering angle up to $\approx 105°$. This large scattering angle region will be covered by two identical modules which form the Large Angle electromagnetic Calorimeter (LAC) provided by the AIACE[1] collaboration of the Istituto Nazionale di Fisica Nucleare (INFN). Each module of the LAC covers a polar angle $\Delta\vartheta \approx 35°$, an azimuth angle $\Delta\phi \approx 55°$ and can be installed either in the same sector, then covering scattering angles up to $\approx 105°$, or in two different sectors covering scattering angles up to $\approx 75°$.

Both the forward and the large angle electromagnetic calorimeters will be used to i) identify electrons at first trigger level, in conjunction with the Cherenkov counters, with 100% efficiency, ii) enhance particle identification by distinguishing pions from electrons, with a rejection factor ≥ 50, iii) enable the detection of photons with energies as low as 20–30 MeV, iv) allow an off line invariant mass reconstruction for π^0 and η with $\delta M_{\pi}^{0} < 20$ MeV and $\delta M_{\eta} < 80$ MeV, v) detect neutrons and measure their momentum.

We found the solution to these design requests in a multi-layer structure which provides the best matching between good energy resolution and high neutron detection efficiency requirements. Each module of the LAC consists of 33 layers each composed by a 2 mm thick lead plate and a 15 mm thick, roughly 10 cm wide plastic scintillators. The bar width increases going from the inner toward the outer side to guarantee the tapering required by CLAS geometry. The scintillators bars in consecutive layers are rotated by 90° with respect to the previous plane, to form a 40×24 matrix of roughly 10×10 cm^2 cells. The area of the surface exposed to particle fluxes is 217×400 cm^2. The longest scintillators strips are about 4.5 m long. Moreover, each module is longitudinally divided into an inner and an outer part to improve the electron–pion

*Corresponding author. Tel. +39 6 9403 2316, fax +39 6 9403 2559, e-mail desanctis@vaxlnf.lnf.infn.it.

[1] AIACE is the acronym for Attività Italiana A CEbaf. It is also the italian name of Aiax, the Iliad hero king of Salamis.

PII S0168-9002(96)00590-6

discrimination. Scintillators lying (for the inner and outer parts separately) one on top of the other with the same orientation form one stack. So for the inner and outer parts separately there are 128 different stacks. The light generated in the scintillators is collected at both scintillator ends, summed separately for each stack in a suitable shaped light guide, and transmitted to the photomultipliers (EMI 9954A) which are positioned on the top surface of the module. The total number of the photomultipliers is, thus, 256 for each module [3].

In spite of the collection of light at both scintillator ends Monte Carlo simulation showed that scintillator bars with light attenuation length longer than 300 cm and fluctuations in the light transmission properties (material inhomogeneities, fluctuations in the surface properties, etc.) not greater than $\pm 5\%$ are needed to achieve a uniform response within 10% over the entire area covered by the LAC. Moreover, fluctuations around average values, handling and ageing of scintillator can also spoil the energy resolution. Then, measurements of light output, light transmission, and propagation time for each scintillator bar were performed to check their fulfilment of the requested specifications.

To satisfy the above requirements NE developed the new high quality plastic scintillator, NE110A [4]. In this paper we report on the performance of the 2128 scintillators (1360 "short" scintillators with length ranging from 217.5 up to 240 cm, and 768 "long" scintillators with length ranging from 401.2 up to 442 cm) of the two modules of the large angle calorimeter. We also present the results of a measurement with cosmic rays of the attenuation length and timing of the scintillators assembled in one stack in the first module.

2. Experimental set-up

A schematic view of the apparatus used in the scintillators tests is shown in Fig. 1. It consists of a 6 m long light-tight box, which houses two plastic scintillator bars at a time, their photomultipliers (EMI 9954A (PM1)), two probe phototubes (Hamamatsu R1450 (PM3)), and a bidirectional collimated radioactive ^{90}Sr β-source (E_{max} = 2.27 MeV). The source and the PM3 probes were mounted on a step motor driven cart that could be moved simultaneously along the scintillator bars.

The light emitted by each scintillator was transmitted to the PM1 via a small ($\approx$1 mm) air gap and also detected by the PM3 located on the opposite side of the scintillator with its photocathode facing the radioactive source. The distance of the probes PM3 to the relevant scintillator surfaces was about 1 mm. To reproduce the real configuration of scintillators inside the module, the end of the scintillator bar opposite to the coupling with the PM1 was not blacked.

We chose a ^{90}Sr β-source because its maximum energy released in 1.5 cm thick plastic scintillators yields a quantity of light, with the direct PMT coupling, approximately equivalent to the energy released by a minimum ionising particle and to the average energy deposited by interacting neutrons with momentum up to 2 GeV/c, when the light is collected with the real light guide system. To this end, pulse height cuts were applied to the probes PM3 to select the high energy part of the β-spectrum.

The electronics of the apparatus consists of two identical channels: one for each scintillator. The PM1 and PM3 signals were analysed by CAMAC LeCroy 2249A ADCs, whose gates were provided by the relevant PM3 signals.

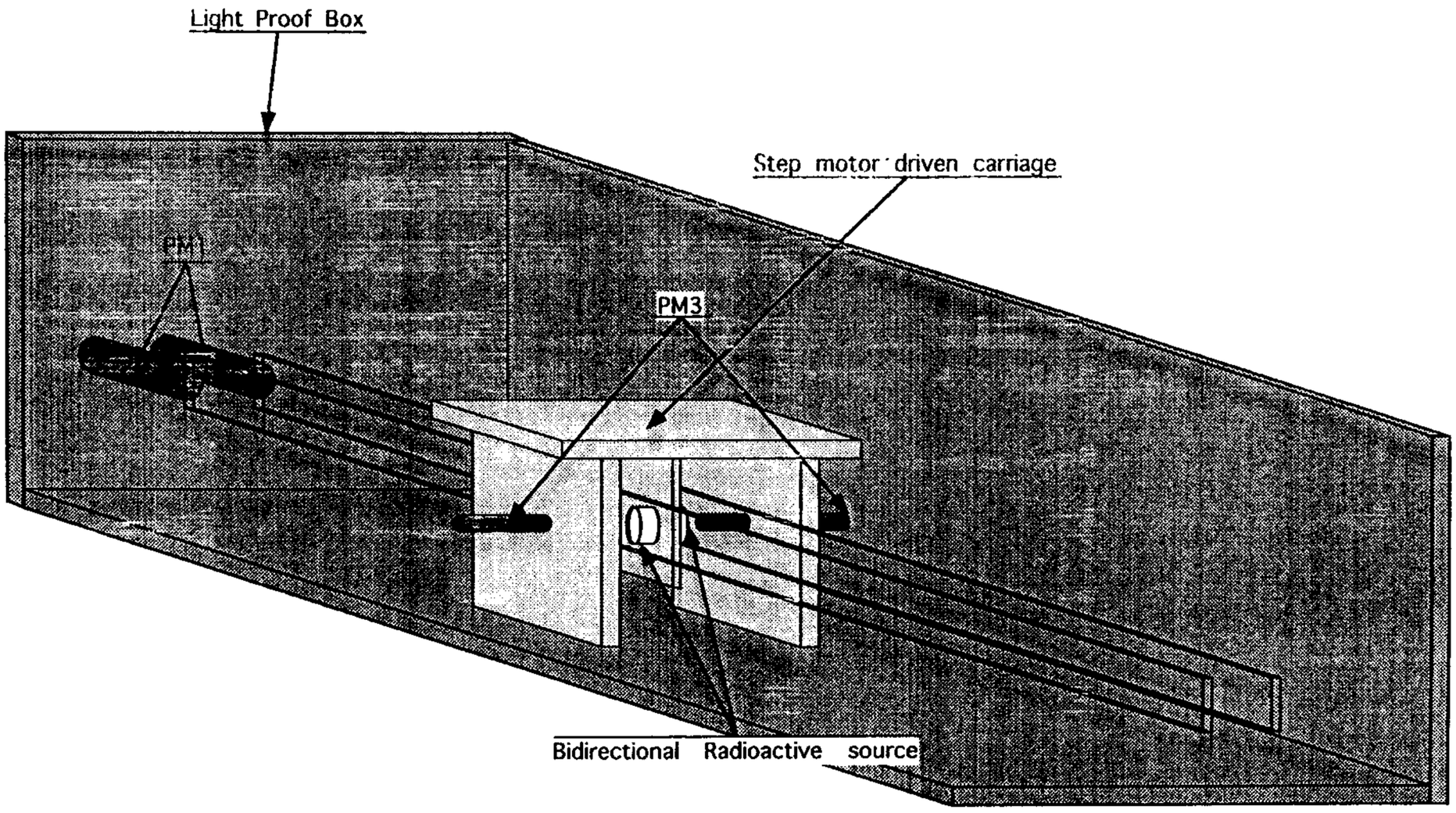

Fig. 1. Schematic view of the apparatus used in the scintillators tests.

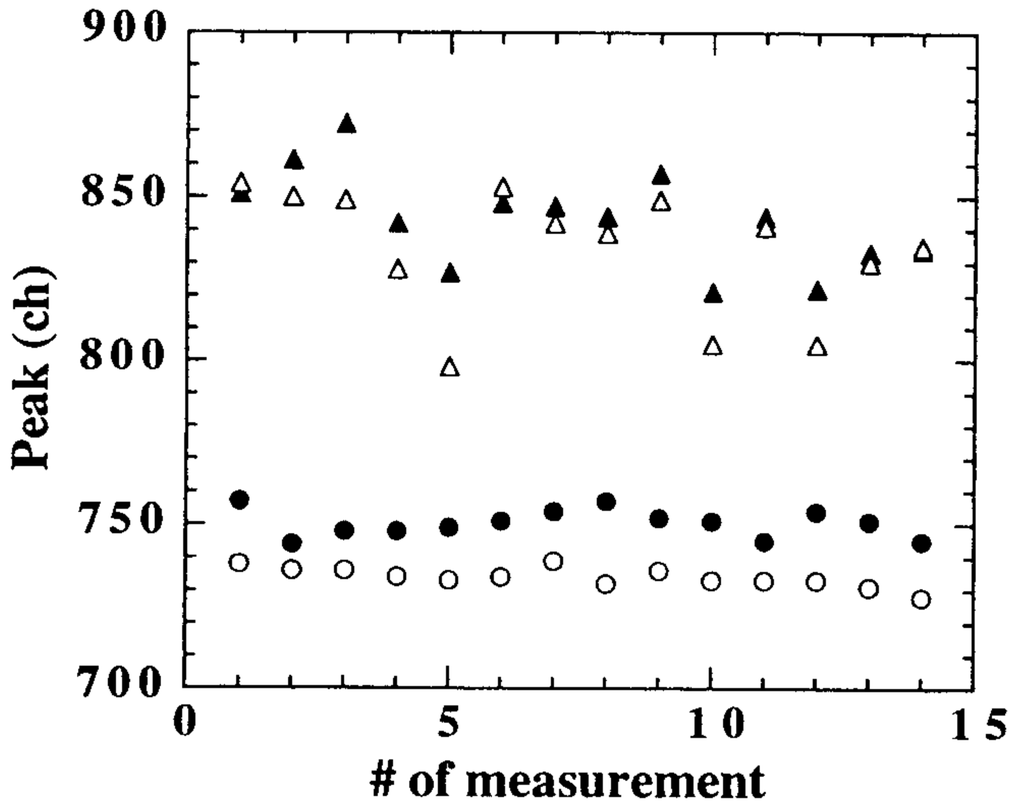

Fig. 2. Stability with the time (4 days) of the PM1's and PM3's peak values of the calibration runs: ▲ PM1 Front; △ PM1 Rear; ● PM3 Front; ○ PM3 Rear. The errors are inside of the point size.

The PM3 and PM1 signals were also discriminated and addressed respectively to the "start" and "stop" inputs of a CAMAC LeCroy 2228A TDC module.

The acquisition program run on a Macintosh computer under the framework of the MacUA1 development system[2].

The acceptance procedure consisted in checking the light output, the attenuation length, the uniformity and the propagation time of the scintillators. Calibration runs were regularly made, in order to check the stability of the apparatus. To this end, we registered the PM1's and PM3's spectra provided by the light emitted by two 20 cm long scintillators positioned at the place of the scintillator bars. The spectra were registered with the source at 10 cm from the PM1. Fig. 2 shows, as an example, the stability of the PM1 and PM3 peak values during four days of test, for both the rear and front chains.

During all the period of the tests (about 2 yr) the variation of the two PM1 and PM3 pairs ranged within ±5% and ±2.5%, respectively.

3. Results

3.1. Attenuation length

For these measurements the source and the probe PM3 were moved, by a computer controlled stepping motor, along the median plane of the scintillators bars, to the fixed test positions (that were 11 and 6 for the long and short scintillator bars, respectively, i.e. one position every 40 cm) and the measured spectra of the PM1 signals were

[2]The MacUA1 system was developed by the on-line team of CERN's UA1 collaboration.

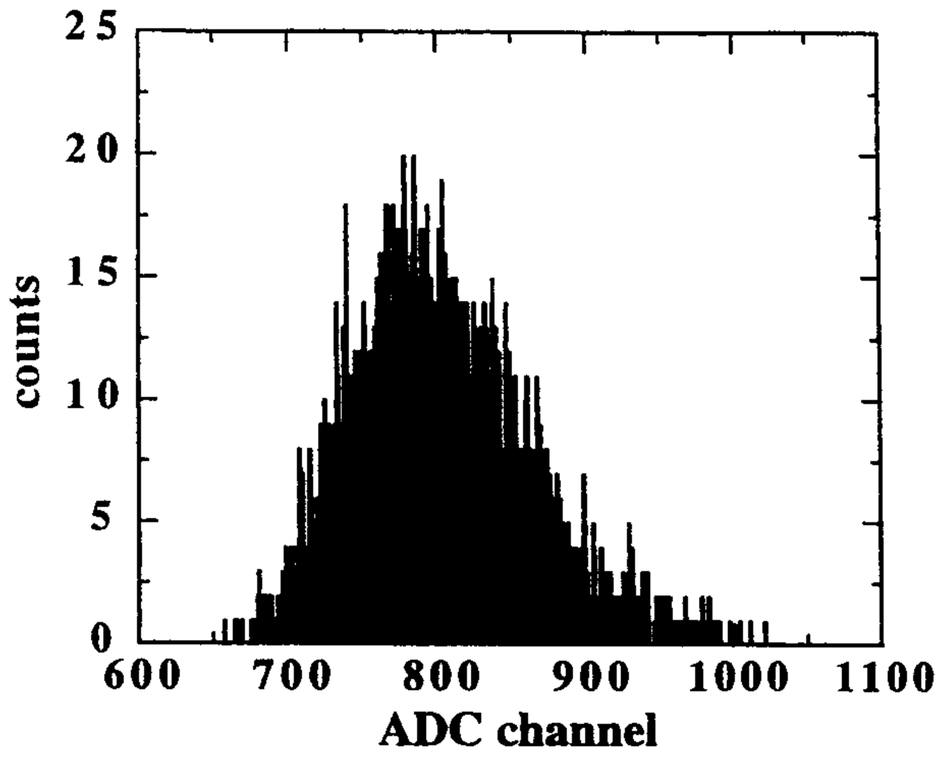

Fig. 3. Typical PM1 ADC spectrum.

registered. A typical spectrum is shown in Fig. 3. The pulse-height spectra measured at each position x were fitted with Gaussian curve and the relevant mean values should be described by a sum of two exponentials

$$A(x) = A_0 e^{-x/\lambda} \lambda_0 + A_1 e^{-x/\lambda_1},$$

where x (cm) is the distance of the source from the PM1, A_0 (A_1) and λ_0 (λ_1) are the amplitude and the attenuation length for the short and long contributions. The relative weight A_1/A_0 strongly depends on the adopted read-out system. λ_0 is of the order of a few centimetres and λ_1 of few meters. The particle energy is obtained, knowing the interaction position x, from the photomultiplier output signal providing that the effective values A_0, A_1, λ_0, λ_1 are used. We found λ_0 depressed by the photomultiplier direct coupling configuration, so only the long component was derived by fitting the data to the single exponential form:

$$A(x) = A_1 e^{-x/\lambda_1}.$$

Typical results are given in Fig. 4a and Fig. 4b, respectively for the "short" and "long" scintillators.

The test was passed if the attenuation length resulted greater than 330 cm. Fig. 5 shows the distribution of the attenuation lengths measured for the 2128 scintillator bars: the mean value and standard deviation of the distribution are 410 and 49 cm, respectively.

3.2. Estimate of the number of photoelectrons

The uncertainty in the calorimetry of electromagnetic showers is determined by various sources. The most important ones are: a) sampling fluctuations, b) leakage fluctuations, c) photo-electron statistics and d) light attenuation fluctuations.

A GEANT simulation of the LAC using a value for the attenuation length of 300 cm, and an electron beam incident perpendicularly on the calorimeter predicts an

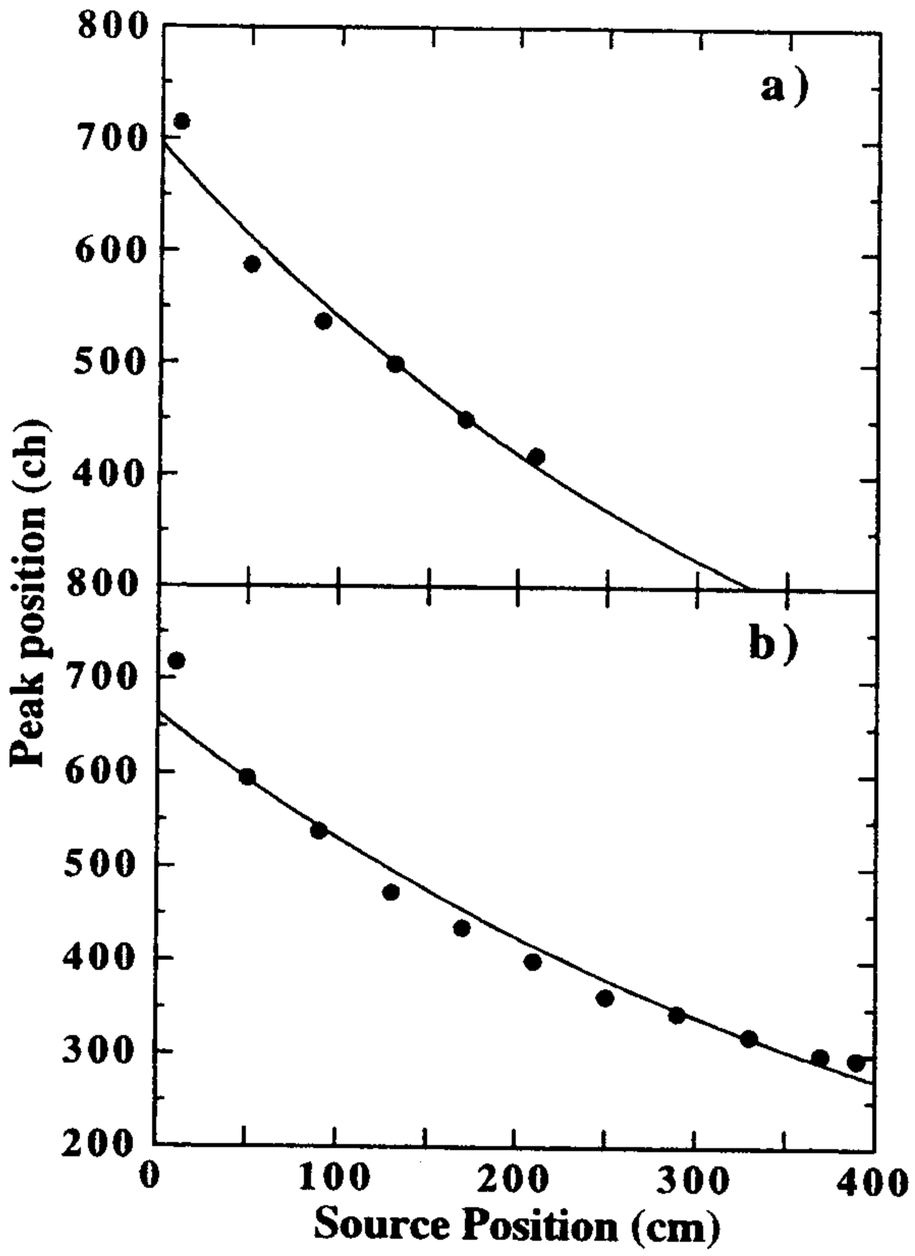

Fig. 4. The single exponential fit (solid line) of the measured mean pulse-height (solid dots) registrated at the chosen test positions along the scintillator: (a) "short" scintillator and (b) "long" scintillator. The errors are inside of the point size.

uncertainty in the energy measurement of $\sim 7\%/\sqrt{E[\mathrm{GeV}]}$, due to the intrinsic sampling fluctuations and leakage fluctuations [5]. An additional uncertainty of $\sim 2.5\%/\sqrt{E[\mathrm{GeV}]}$ comes from photo-electron statistics if ~5 photo-electrons/MeV are collected on the photocathode of the PMT. So, considering that with the final light collection system, made of a lucite light guide [6], the light output will be reduced by a factor about 8, the minimum number of photoelectrons, n_{pe}, per 1 MeV of energy deposition at 10 cm from the PM1, is ≈ 40.

To measure the light yield of each scintillator bar we used the PM1 spectra registered for the attenuation length measurements. In principle, to estimate n_{pe} it suffices to measure the PM1 spectrum at 10 cm, if the particles entering the scintillator are monochromatic. In fact, the amplitude to width ratio of the Gaussian curve which fits the PM1 ADC spectrum is related to this number since the centroid P of the curve is proportional to n_{pe}, while its width increases with $\sqrt{n_{pe}}$. So we can write:

$$\left(\frac{\sigma}{P}\right)^2_{\mathrm{stat}} = \frac{1}{n_{pe}} = \frac{K}{P}, \tag{1}$$

where K is a constant.

In our case the source is not monochromatic and then relation (1) transforms in:

$$\frac{\sigma}{P} = \sqrt{\frac{K}{P} + T}, \tag{2}$$

where the term T accounts for the energy spread of the source. In our case the latter is fixed by the PM3 pulse height cut. Therefore, we derived the values (σ/P) versus the value of the PM1 peak for all the spectra measured at the established positions along the scintillator for a PM3 threshold fixed and stable within $\pm 5\%$.

A typical fit is shown in Fig. 6 where it is reported the ratio σ/P of the PM1 spectrum for a long scintillator as a function of the PM1 peak measured at the chosen test positions. From the fit we obtained the values of the two free parameters K and T and then we extracted the number n_{pe} of photoelectrons at 10 cm using the relation $n_{pe} = P_{10\ \mathrm{cm}}/K$. From these calculations we also found that the total resolution varies from 12% at $x = 10$ cm to 16% at $x = 400$ cm: the contribution of the T term is constant and

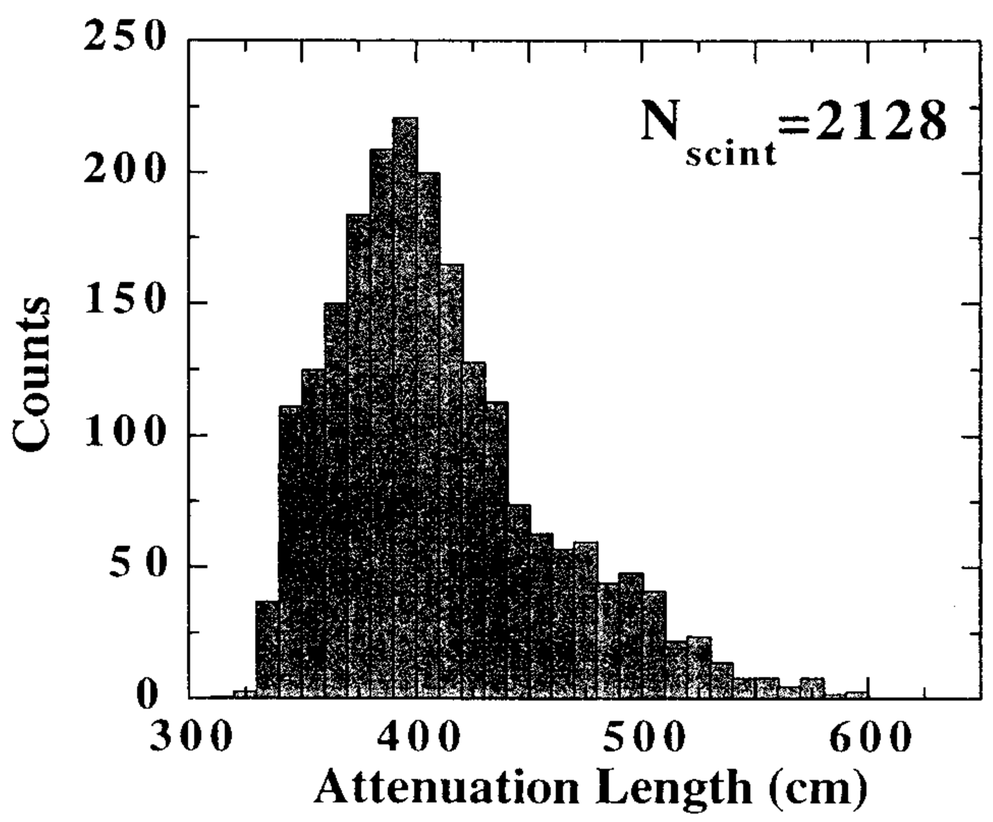

Fig. 5. Distribution of the attenuation lengths for the 2128 scintillators.

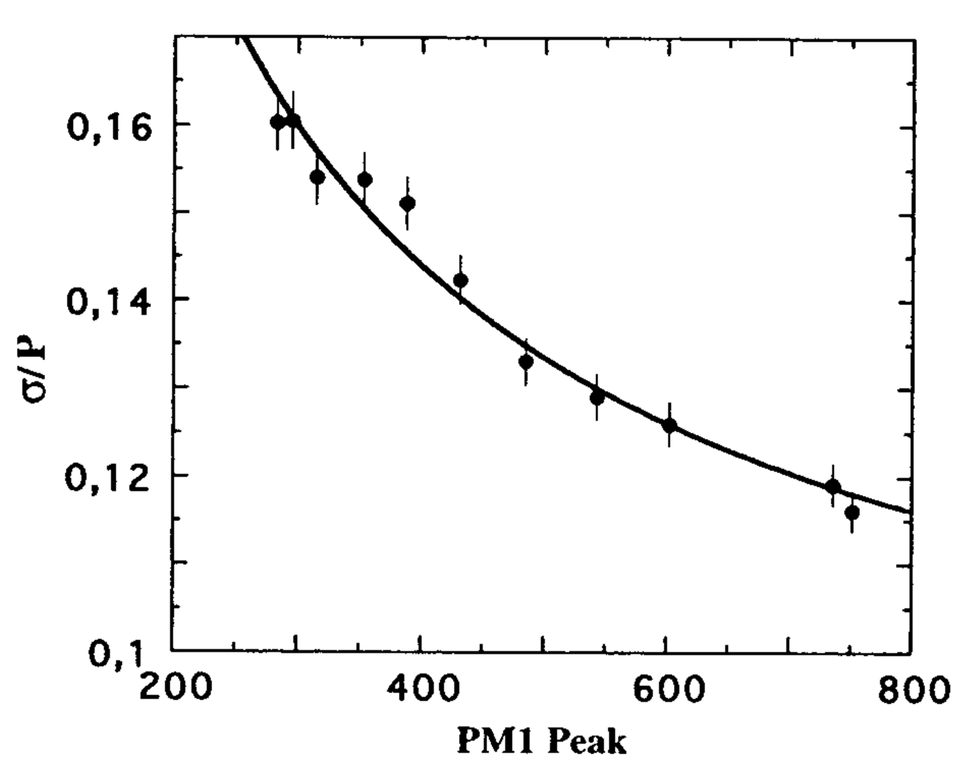

Fig. 6. The ratio σ/peak versus the mean pulse-height (peak) of the PM1 spectra are reported for all the positions measured along the scintillator. The curve is a fit of data to the expression $y = \sqrt{K/\mathrm{peak} + T}$.

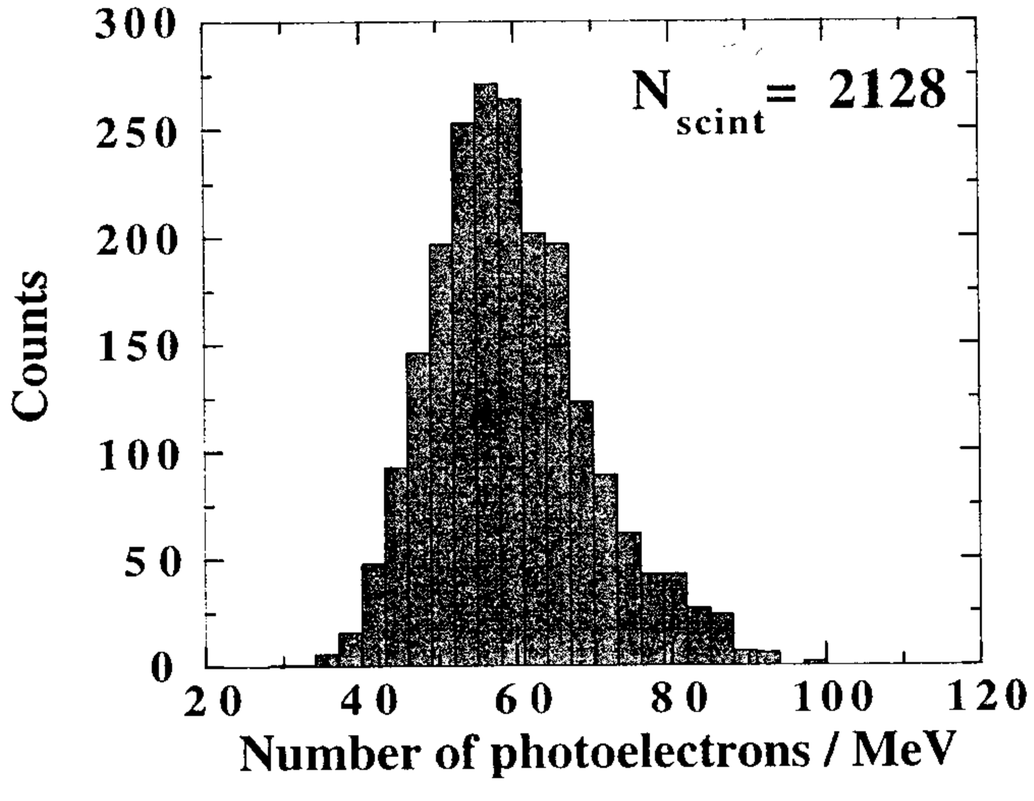

Fig. 7. Distribution of the number of photoelectrons/MeV.

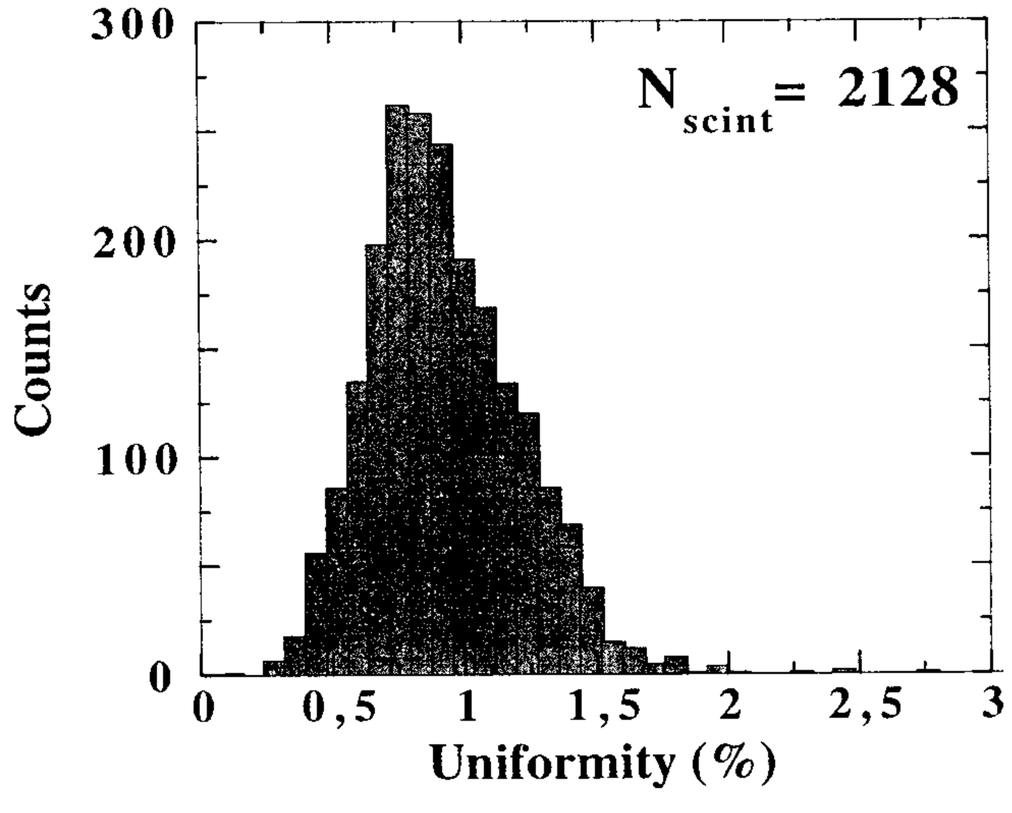

Fig. 8. Distribution of the ratio Δpeak/peak for the PM3 signal along the scintillator.

equal to ≈8%, while the one of the term K/P varies from ≈9% to 14%.

Fig. 7 shows the distribution of the number of photoelectrons per MeV of deposited energy. The distribution has a mean value of 59±10: then 98% of the scintillators fulfil the request.

3.3. Uniformity

The light generated in the scintillators will be collected at both scintillator ends, summed separately for each stack in a suitable shaped light guide [6], and transmitted to the photomultiplier; so a uniform response of the calorimeter is important.

The PM3 signal allowed to measure the light emitted at the different positions along the scintillator bars for the same energy deposition. This quantity is proportional to the product of the local thickness and efficiency of the scintillator bar. Since the thickness is constant within ±0.5 mm, a uniform response of the PM3 signal means a constant scintillation efficiency.

To test the uniformity of the scintillator response we measured the peak values for the PM3 signal along each scintillator and required a ratio of $\Delta P/\langle P\rangle \leq 5\%$, being $\Delta P = P_{max} - P_{min}$ and $\langle P\rangle = (P_{max} + P_{min})/2$.

In Fig. 8 we show the distribution of these ratios for all the 2128 scintillators which has a mean value of (0.9±0.3)%.

3.4. Propagation time

The electromagnetic shower calorimeter will be the CLAS most sensitive detectors to neutrons. When a neutron collides with a nucleus of the detector some of the neutron energy can be transmitted to particles that are easily detected by the electromagnetic shower calorimeter. A measured time and a deposited energy can then be determined for those neutrons that interact in the detector. The energy deposition is typically not sufficiently correlated to the incident neutron energy to be used as a measure of the incident neutron energy. The time of flight measurement of the neutrons from the target to the calorimeter is the most accurate way to determine the neutron energy. Then the timing characteristics of the electromagnetic calorimeter are important.

We have measured the propagation time of the light pulse in the scintillator bars. The PM3 signal was sent to the "start" input of a TDC CAMAC module, while the PM1 signal was sent to the "stop" input of the TDC.

In Fig. 9 the propagation time of the light from 2 MeV electrons versus the distance is reported: points represent the mean values of the Gaussians which well reproduce the distributions and the error bars represent the variance of the distributions. In the scintillators used an effective velocity of ≈16 cm/ns was obtained. This is 16% less than the actual speed of light in scintillator (19 cm/ns) so

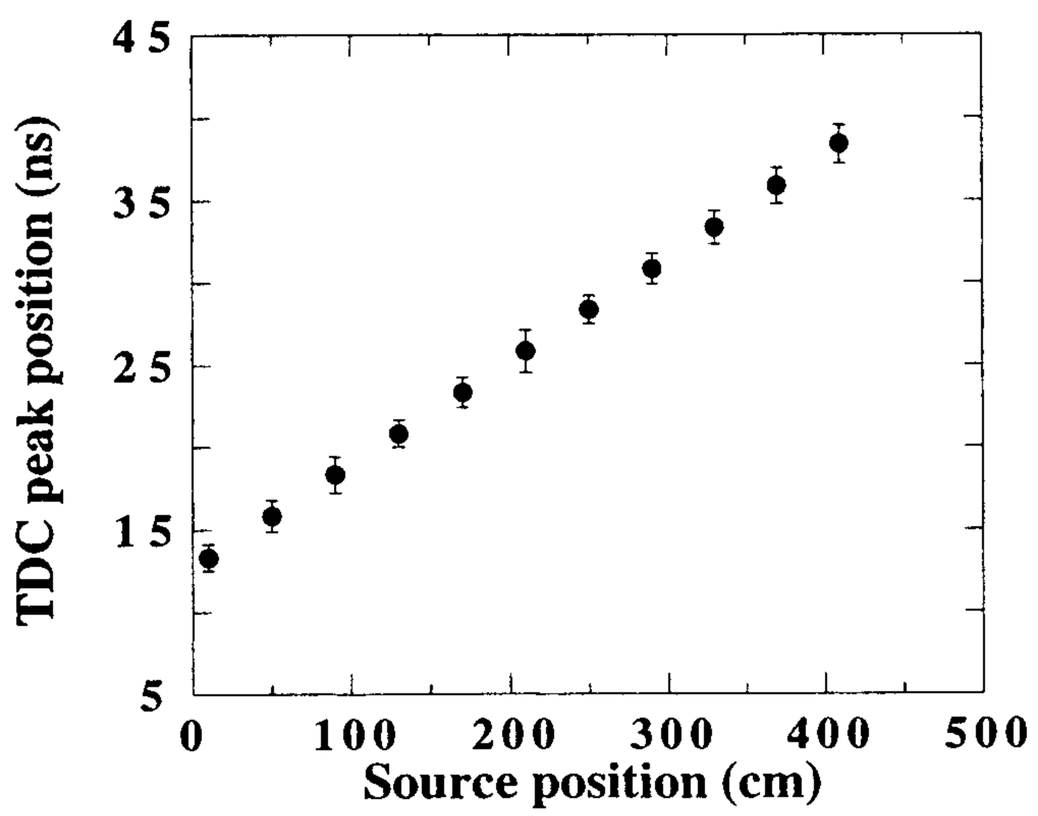

Fig. 9. Time propagation of the light from 2 MeV electrons versus the distance (the distribution is Gaussian and the error bars of the points represent the width of the distribution).

the average path length is 16% greater than a straight path inside the scintillator.

4. Tests with cosmic muons

Light transmission and time propagation of the scintillator bars, have been also measured in the first assembled module using cosmic muons. We placed a trigger scintillation counter, $30\times30\times1$ cm^3 size, in the module focus (which is the target position in the CLAS spectrometer) to selected only the cosmic rays that crossed the module through a single stack.

In Fig. 10 are reported the ADC mean values of the signals collected at both ends of one stack versus the position along the scintillators. In the figure are also shown the average of the values obtained for the 8 scintillators of the stack during the acceptance measurements. As we see the agreement is very good; the slight difference at ≈ 10 cm is due to the different coupling between the scintillators and the PMT used in the two measurements: a direct coupling during the acceptance tests, a light guide between the PMT and the scintillators during the cosmic muon measurement.

The total energy deposited in the considered stack, which was determined as 2 times the squared root of the product of the signals collected at both scintillator ends, is also shown in the figure. As we can see the response is uniform within 10%, as requested. The solid line in the figure is a fit of the data to the function

$$A(x) = A_0\left[e^{-x/\lambda} + \alpha e^{-(2L-x)/\lambda}\right],$$

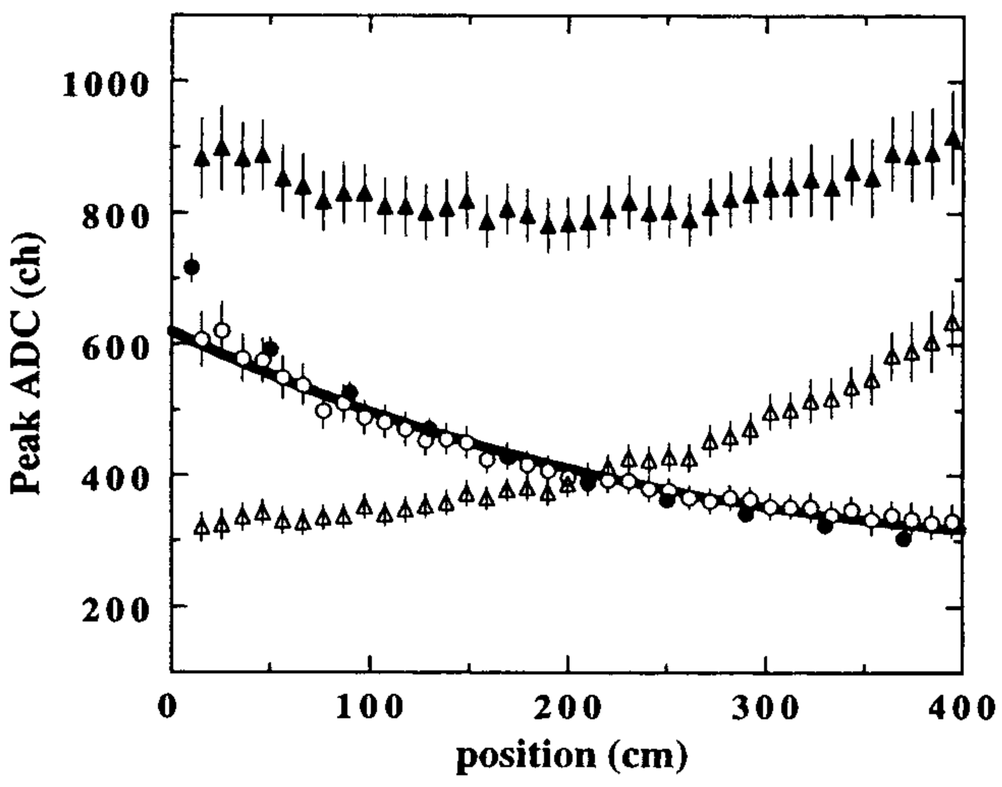

Fig. 10. Experimental values, obtained during the cosmic muon tests, of the signal collected for one stack at both ends (open triangles and open circles) versus the position along the scintillators (the solid line is a fit of the data). The solid triangles represent the total energy deposited in the stack. The solid circles are the signal mean values obtained during the acceptance tests at the NE.

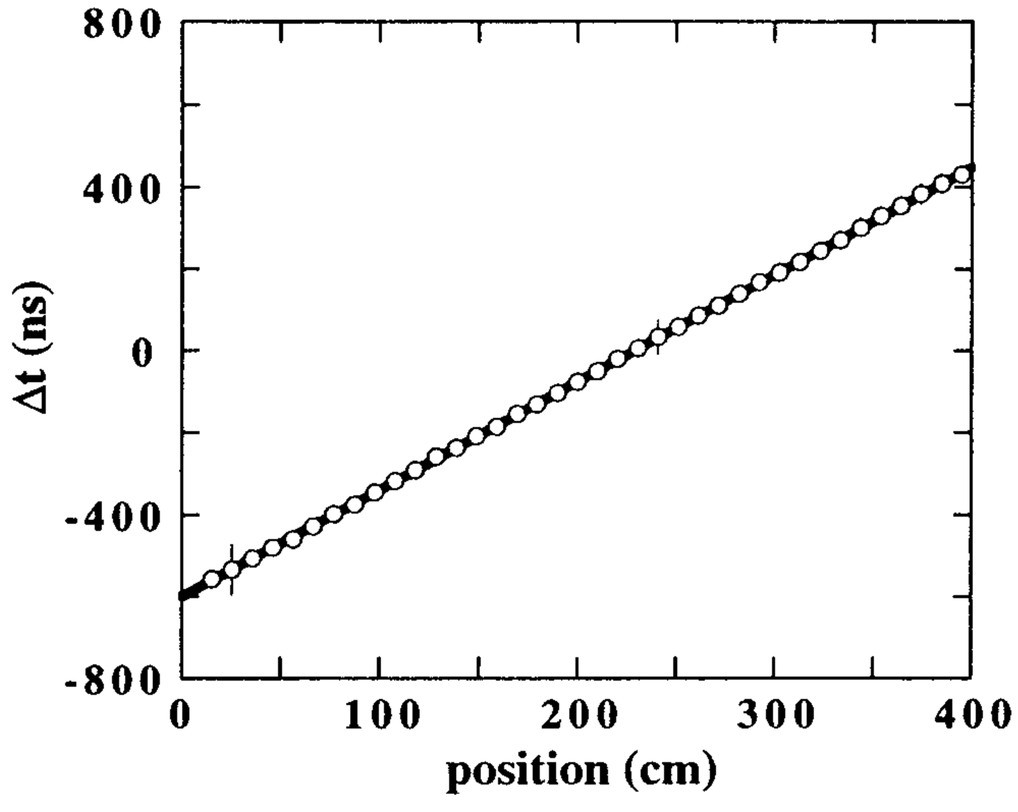

Fig. 11. Timing response of the scintillator stack measured with cosmic muons. The solid line is a linear fit of the data.

where L is the length of the scintillator and α is the fraction of the emitted light reflected back to the photomultiplier at the scintillator end opposite to the PMT: this function can be used for a software position correction procedure to further improve the uniformity and then the resolution of the detector.

The linearity of the timing response of the same scintillator stack, has been also measured. In Fig. 11 is shown the difference between the transit time, Δt, of the signal collected at both ends of the stack when a cosmic ray pass through the different position along the scintillators. Since Δt is related to the velocity of the light in the scintillators through the simple relation

$$\Delta t = \frac{2x}{v} + \text{const.},$$

where x is the position along the scintillators and v is the velocity of the light, from the slope of the linear curve (solid line) which fits the experimental points, we extracted the value $v = 15.7$ cm/ns, which is in good agreement with the value obtained from the acceptance tests.

5. Conclusions

We reported the characteristics of the 2128 NE110A plastic scintillators for the two modules of the AIACE large angle electromagnetic calorimeter. Attenuation length, light output, uniformity and light propagation time were measured. A ^{90}Sr β-source has been used to simulate minimum ionising particles and interacting neutrons. The results showed a very good attenuation length ($\approx$400 cm), a light output of $\geq$40 photoelectrons/MeV and a very good uniformity ($>$98%).

Acknowledgments

We thank dr. T. Hanson and dr. H. Hunter for the warm hospitality at the NE Technology and the Frascati technical staff, A. Orlandi, W. Pesci, G. Serafini and A. Viticchié for the continuing assistance in all stages of the apparatus construction and scintillator tests. We thank also Mr. M. Castoldi, P. Cocconi and F. Parodi from INFN Genova for useful discussions on the technical details of the test apparatus.

References

[1] J.J. Domingo, Proc. 5th Workshop on Perspectives in Nuclear Physics at Intermediate Energies, Trieste May 6–10, 1991, eds. S. Boffi, C. Ciofi degli Atti and M. Giannini (World Scientific, 1992) p. 260.

[2] V.D. Burkert and B.A. Mecking, in: Modern Topics in Electron Scattering, eds. B. Frois and I. Sick (World Scientific, 1991).

[3] M. Taiuti et al., INFN Genova Internal Report, INFN/BE-95/03 (1995).

[4] M. Taiuti et al., Nucl. Instr. and Meth. A 370 (1996) 429.

[5] V.I. Mokeev et al., INFN Genova Internal Report, INFN/BE-95/02 (1995).

[6] M. Taiuti et al., Nucl. Instr. and Meth. A 357 (1995) 344.